Sliding IPL: An efficient approach for estimating the phases of large SAR image time series

Dana El Hajjar[1,3], *Arnaud Breloy*[2], *Guillaume Ginolhac*[1], *Mohammed Nabil El Korso*[3], and *Yajing Yan*[1]

[1]Université Savoie Mont Blanc, LISTIC, F-74000 Annecy, France
[2]Conservatoire national des arts et métiers, CEDRIC, Paris, France
[3]Université Paris-Saclay, CentraleSupélec, L2S, Gif-sur-Yvette, France

***Abstract*—Thanks to missions like Sentinel-1, with their short revisit time (e.g. 6-12 days), a vast amount of Synthetic Aperture Radar (SAR) images is now available. This abundance is advantageous for the accessibility of time series and their subsequent processing such as Multi-Temporal Interferometric SAR (MT-InSAR) that allows for precise monitoring of land motion. However, it poses challenges in managing such large datasets efficiently while aiming to use them in a resource-conscious and cost-effective manner. This contribution introduces a novel Interferometric Phase Linking (IPL) approach for SAR images eliminating the need to store all past acquisitions while still leveraging their information. The method involves sliding a temporal window over the time series, allowing the integration of new SAR acquisitions. This approach is faster than traditional IPL methods, whether applied offline or sequentially. Its validity is demonstrated using a Sentinel-1 SAR image time series to monitor Mexico City.**

***Index Terms*—phase estimation, covariance matrix estimation, sliding temporal window, SAR image, Interferometric Phase Linking**

I. Introduction

In the past decade, Interferometric SAR (InSAR) has undergone several updates and advancements in the field of Earth monitoring, particularly for monitoring land motion. Seminal methods began with the simple comparison of two SAR images of the same scene acquired at different dates (2-pass InSAR). However, this approach reached its limits when the time interval between the two acquired images becomes too large, leading to a loss of valuable information due to signal decorrelation. Subsequently, Multi-Temporal Interferometric SAR (MT-InSAR) approaches demonstrated significant improvements over 2-pass InSAR by leveraging time series of SAR images. One pivotal technique in MT-InSAR, called Interferometric Phase Linking (IPL), aims at estimating the phase differences within the time series by exploiting the expected phase structure of the Covariance Matrix (CM) of local pixel patches. A seminal IPL algorithm was proposed in [1], deriving an approximate Maximum Likelihood Estimator (MLE) of the phases of the CM under the Gaussian assumption. This approach relies on a plug-in estimate of the coherence matrix (approaches aiming for a joint estimation were proposed in [2, 3]). This algorithm led to many variants: overviews of the existing MLE-type IPL algorithms can be found in [4, 5]. Recently, a unification was proposed in [6] through the prism of a covariance fitting formulation: the main idea being to restore the expected InSAR phase structure from any plug-in estimate. This paradigm includes the aforementioned MLEs as special case, but allows for many generalizations (fitting matrix distance, CM plug-in, regularization) that were shown to be beneficial in terms of either estimation performance or computational complexity [6–8].

Processing large SAR image time series is now becoming increasingly complex: most IPL methods rely on computationally expensive mathematical operations applied to CM, whose size grows with each new acquisition. Traditional approaches are not well-suited to integrate new images efficiently without having to re-run the entire algorithmic process on the whole data. In practice, this means repeatedly estimating large CM and processing a massive volume of images each time a new image is added to the time series. This issue could be addressed by developing new efficient sequential IPL algorithms, which, to the best of our knowledge, has not been extensively studied in the literature. The few existing approaches rely on processing temporal blocks within the time series. The sequential estimator proposed in [9] consists of dividing the SAR image time series into mini-stacks and performing IPL within each one, to obtain a compressed version, i.e virtual interferogram of each mini-stack. The re-calibration of each phase of the whole time series is obtained by performing a global IPL on compressed versions of each mini-stack. This two-step approach is sub-optimal and prone to error accumulation. Another sequential methodology was proposed in [10, 11], allowing the integration of a single new SAR acquisition at a time. This method builds a sequential MLE in order to estimate only the parameters related to the new image (variance, phase and coherence with historical images), while leveraging the estimations already performed on past images. The process has been extended to the covariance fitting framework of [6] in [12], which allowed for the sequential integration of new mini-stacks of images at once. Both approaches [10, 11] and [12] achieve an accuracy similar to traditional offline methods. However, they require to keep the historical images and previous estimates of the CM, which still hold major limitations in terms of computational load.

This work is funded by the ANR REPED-SARIX project (ANR-21-CE23-0012-01) of the French National Agency of Research. The source code is available on GitHub at https://github.com/DanaElhajjar/Sl-IPL.

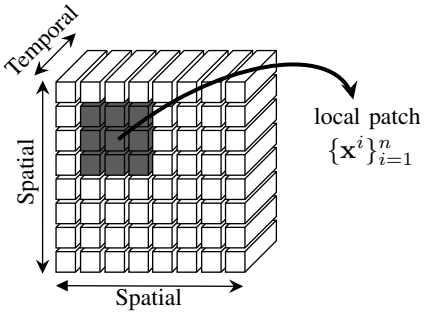

Fig. 1. Stack of P co-registered SAR images where the local patch $\{\mathbf{x}^i\}_{i=1}^n$ is represented in gray.

In this work, we propose a novel sequential IPL method that overcomes the aforementioned issues. It involves sliding a temporal window over the time series, allowing for the integration of new SAR acquisitions. For each mini-stack covered by the sliding window, we construct a regularized IPL estimation problem involving a penalty term that preserves historical information. The methodology is quite generic and suited to any IPL formulation. In this paper, we focus on the least-squares covariance fitting IPL of [6], for which we derive a Majorization-Minimization (MM) algorithm. The validity of the proposed method is then demonstrated using a Sentinel-1 dataset to monitor the subsidence of Mexico City.

II. SAR images time series model

For a given stack of P co-registered SAR images, we consider a sliding spatial window of n pixels which corresponds to the homogeneous spatial neighborhood denoted $\{\mathbf{x}^i\}_{i=1}^n$, i.e. $\mathbf{x}^i \in \mathbb{C}^P$, for all $i \in [\![1, n]\!]$. Each pixel of the local patch

$$\mathbf{x}^i = [x_1^i, \dots, x_P^i]^T \in \mathbb{C}^P \tag{1}$$

contains a time series of P images (see Fig. 1). The first and second order moments are as follows

$$\mathbb{E}(x_m) = 0,\ \forall\ m \in [\![1, P]\!] \tag{2}$$

$$\mathbb{E}(x_m (x_q)^*) = \nu_{mq}\sigma_m\sigma_q e^{j(\theta_m - \theta_q)},\ \forall\ (m, q) \in [\![1, P]\!]^2 \tag{3}$$

The quantity $\nu_{mq} \in [\![0, 1]\!]$ denotes the coherence between the pixel x_m and x_q, $\sigma_m, \sigma_q \in \mathbb{R}^+$ corresponds to the standard deviation of the pixel x_m and x_q respectively. θ_m, θ_q are the phases at instant m and q, and j is the imaginary unit. The covariance between the pixels is thus complex-valued, and its magnitude depends on the standard deviations and the coherence, while its phase difference is determined by the difference in phases of SAR images. The corresponding matrix notation of the covariance is as follows

$$\mathbf{\Sigma} = \mathbf{\Psi} \odot \mathbf{w}\mathbf{w}^H \tag{4}$$

where $\mathbf{\Psi}$ denotes the coherence matrix and $\mathbf{w}$ is the vector containing the exponential of the complex phases, i.e. $\mathbf{w} = [e^{j\theta_0}, \dots, e^{j\theta_P}] \in \mathbb{T}_P$, where

$$\mathbb{T}_P = \{\mathbf{w} \in \mathbb{C}^P \,|\, |[\mathbf{w}]_i| = 1, \forall i \in [1, P]\} \tag{5}$$

is the P-torus of phase only complex vector.

III. Interferometric Phase Linking

IPL algorithms aim to estimate the phase differences of a time series of SAR images, i.e. recovering $\mathbf{w}$, from the set $\{\mathbf{x}^i\}_{i=1}^n$ by leveraging the assumed CM structure in (4). In this section, we detail existing methods that operate in both offline and sequential modes, respectively.

A. Offline IPL

Exploiting in an offline way the CM of the whole time series allows us to make use of all possible combinations of phase differences in (3). To estimate $\mathbf{w}$, from the set $\{\mathbf{x}^i\}_{i=1}^n$, we consider the COvariance Fitting Interferometric Phase Linking (COFI-PL) formulation of [6]. The vector $\mathbf{w}$ is estimated such it that provides the "best fit" between a plug-in estimate of the CM $\hat{\mathbf{\Sigma}}$ (built form $\{\mathbf{x}^i\}_{i=1}^n$) and its structure in (4). The general form of the COFI-PL problem thus reads as follows

$$\begin{aligned} \underset{\mathbf{w}}{\text{minimize}} \quad & f_{\hat{\mathbf{\Sigma}}}^d(\mathbf{w}) \triangleq d^2(\hat{\mathbf{\Sigma}}, \hat{\mathbf{\Psi}} \circ \mathbf{w}\mathbf{w}^H) \\ \text{subject to} \quad & \theta_1 = 0 \\ & \mathbf{w} \in \mathbb{T}_P \end{aligned} \tag{6}$$

where d stands for any matrix distance. An interesting special case comes form choosing the Sample Covariance Matrix (SCM) $\hat{\mathbf{\Sigma}} = \mathbf{S} = \sum_{i=1}^n \mathbf{x}_i\mathbf{x}_i^H/n$ as a plug-in estimate, and setting d as the Kullback-Leibler (KL) divergence between two Gaussian distributions. These settings in (6) yield (after matrix manipulations) the following objective function

$$f_{\mathbf{S}}^{KL}(\mathbf{w}) = \mathbf{w}^H(\mathrm{mod}(\mathbf{S})^{-1} \circ \mathbf{S})\mathbf{w}. \tag{7}$$

This formulation corresponds the MLE estimator from [1], which motivated many subsequent developments (see overviews in [4, 5]). In this paper, we will build upon the recent advances brought by [6–8, 13] for setting d and $\hat{\mathbf{\Sigma}}$ in the rest of this paper.

1) Choice of matrix distance d: Though any distance metric could be considered, we will rely on the Euclidean distance, as it demonstrated the best empirical results for IPL in [6, 7, 13]. This distance is defined as $d_E^2(\mathbf{A}, \mathbf{B}) = ||\mathbf{A} - \mathbf{B}||_2^2$, which, when used in (6), reduces to

$$f_{\hat{\mathbf{\Sigma}}}^{\mathrm{E}}(\mathbf{w}) = -2\mathbf{w}^H(\mathbf{\Psi} \circ \hat{\mathbf{\Sigma}})\mathbf{w}. \tag{8}$$

A notable advantage of the Frobenius norm over the KL divergence is that it eliminates the need of the CM inversion, thus, reduces the computational load.

2) Choice of the plug-in estimate $\hat{\mathbf{\Sigma}}$: In this work, we consider a robust estimator called Phase-Only Sample Covariance Matrix (PO) [14], which demonstrated significantly superior performance when compared to the SCM in [6]. The estimate is defined as

$$\hat{\mathbf{\Sigma}}_{PO} = \frac{1}{n}\sum_{i=1}^{n} \mathbf{y}^i\mathbf{y}^{iH} \tag{9}$$

where $\mathbf{y} = \Phi_{\mathbb{T}}(\mathbf{x})$ and $\Phi_{\mathbb{T}} : x = re^{i\theta} \to e^{i\theta}$. Furthermore, we apply a tapering matrix [15], as it was shown to be beneficial for IPL in [6–8]. Specifically, CM tapering involves setting the covariance between two dates to zero when their time

difference exceeds a certain threshold b, referred to as the bandwidth. The tapering operator is defined as

$$[\mathbf{W}(b)]_{ij} = \begin{cases} 1 & \text{if} \quad |i-j| \leq b \\ 0 & \text{otherwise.} \end{cases} \tag{10}$$

The regularized estimator has, then, the following form:

$$\hat{\mathbf{\Sigma}}_{BW-PO} = \mathbf{W}(b) \circ \hat{\mathbf{\Sigma}}_{PO}. \tag{11}$$

To conclude, the baseline for offline IPL will be produced in this paper by solving (6) with fitting cost $f^{\mathrm{E}}_{\hat{\mathbf{\Sigma}}}$ in (8) and plug in estimate $\hat{\mathbf{\Sigma}}_{BW-PO}$ in (11).

B. Sequential IPL

When a new SAR acquisition is integrated, the size of the data vector increases (with one or more components being added), as well as the CM. Integrating this new data in offline IPL formulations requires solving (6) for all pixel patches, and working on CM of increased dimension. The process in computationally demanding, so several works addressed the issue by developing sequential methods.

1) Sequential IPL from [9]: This method involves dividing the SAR image time series into independent mini-stacks on which IPL is performed separately. This is followed by compressing each mini-stack into a virtual interferogram, on which a global IPL is applied to calibrate the phase estimates obtained in the first step. This two-step approach involving a calibration post-processing appears to be sub-optimal and prone to error accumulation over time. Furthermore, this approach still requires storing the compressed interferograms and processing data of increasing dimension, which limits its widespread application

2) Sequential IPL from [12]: This method builds upon the formulation (6) to integrate a mini-stack of m new SAR images. The new stack yields a time series that can be expressed in block form as $\mathbf{x} = [\mathbf{x}_{\text{old}}^\top, \mathbf{x}_{\text{new}}^\top]^\top$, and whose CM is still structured as in (4) with phase vector $\mathbf{w} = [\mathbf{w}_{\text{old}}^\top, \mathbf{w}_{\text{new}}^\top]^\top$. Integrating new mini-stacks over time then yields a sequence of problems of the form

$$\begin{array}{ll} \underset{\mathbf{w}_{\text{new}}}{\text{minimize}} & f^d_{\hat{\mathbf{\Sigma}}}(\mathbf{w}) \\ \text{subject to} & \mathbf{w} = [\mathbf{w}_{\text{old}}^\top, \mathbf{w}_{\text{new}}^\top]^\top \\ & \mathbf{w}_{\text{new}} \in \mathbb{T}_m \end{array} \tag{12}$$

which can be efficiently solved in practice. This method allows for achieving similar performance to offline IPL but at a lower computational cost. However, this approach requires keeping and storing the entire time series images (both historical and newly acquired ones), as well as the corresponding CM and phases.

IV. Sliding IPL

The previous overview showed that certain limitations remain in the state-of-the-art sequential IPL, particularly in terms of storage and computational efficiency. In the next section, we present a novel approach that addresses these challenges.

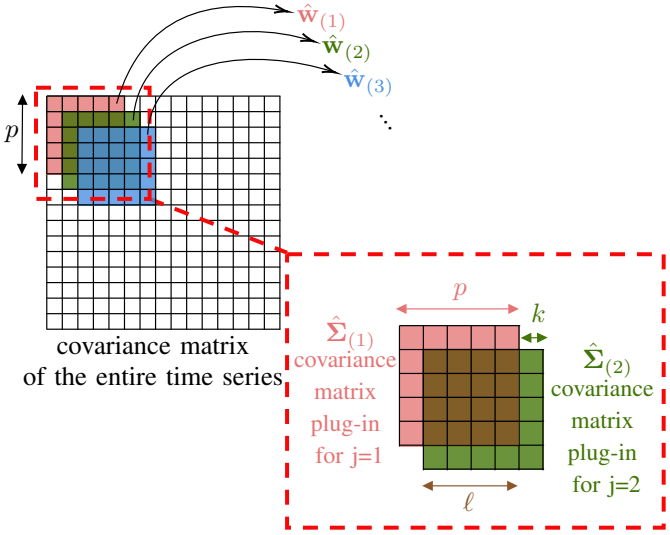

Fig. 2. Representation of the CM of the entire time series of SAR images with a temporal window of size p, a stride k and an overlap ℓ. The exponential phases vector of the stack (j) is presented by $\hat{\mathbf{w}}_{(j)}$, and the corresponding CM plug-in by $\hat{\mathbf{\Sigma}}_{(j)}$.

A. Methodology

The main idea of the proposed method is to slide a temporal window of size p with a stride k, resulting in an overlap of size $\ell = p - k$, as illustrated in Fig. 2. In this setup $\hat{\mathbf{w}}_{(j)}$ denotes the estimated phases vector of each temporal stack, and $\hat{\mathbf{\Sigma}}_{(j)}$ the corresponding CM plug-in. The common part between the estimated phase vectors of the stack $(j-1)$ and the stack (j), is denoted as $\mathbf{w}_{\ell(j-1)}$, which is a vector of size ℓ. We then propose to solve the sequence of regularized IPL problems, defined as

$$\begin{array}{ll} \underset{\mathbf{w}_{(j)}}{\min} & f^{\mathrm{E}}_{\hat{\mathbf{\Sigma}}}(\mathbf{w}_{(j)}) + \lambda h(\mathbf{w}_{(j)}) \\ \text{s.t.} & \mathbf{w}_{(j)} \in \mathbb{T}_p. \end{array} \tag{13}$$

where h is a penalty term that guarantees the phase estimates to stay close to the previous ones within the window overlap. In this work, we focus on the squared-distance regularization

$$h(\mathbf{w}_{(j)}) = \left\| \begin{pmatrix} \mathbf{w}_{\ell(j-1)} \\ \mathbf{0} \end{pmatrix} - \mathbf{w}_{(j)} \right\|^2$$

whose efficiency will be demonstrated in the experiment section. We also emphasis that the choice of λ appears not to be critical, as we observed in our experiments that the obtained solutions were quite stable within the range of tested parameters. A notable feature of this sliding method is that it eliminates the need to store all the historical images outside of the overlap. Hence, each optimization problem in the sequence remains of constant size p.

B. Algorithm

We propose a MM algorithm [16] to solve the optimization problem (13). The first step of the MM algorithm, called

"Majorization", consists of finding the surrogate function $g(.|\mathbf{w}^{(t)})$ that majorizes the objective function $f(\mathbf{w})$.

$$f(\mathbf{w}) \leq g(\mathbf{w}|\mathbf{w}^{(t)}), \quad \forall\, \mathbf{w} \in \mathbb{T}_p \tag{14}$$

with equality $f(\mathbf{w}^{(t)}) = g(\mathbf{w}^{(t)}|\mathbf{w}^{(t)})$.

Lemma 1 *The concave quadratic form*

$$f : \mathbf{w} \mapsto -\mathbf{w}^H \mathbf{H}\mathbf{w}$$

is majored, with equality at point $\mathbf{w}^{(t)}$*, by*

$$g(\mathbf{w}|\mathbf{w}^{(t)}) = -2Re(\mathbf{w}^H \mathbf{H}\mathbf{w}^{(t)})$$

Using Lemma 1, the cost function in the problem (13) can be majored by the surrogate function

$$g(\mathbf{w}_{(j)}|\mathbf{w}_{(j)}^{(t)}) = -\mathrm{Re}\Bigg(\mathbf{w}_{(j)}^H \underbrace{\left[4(\hat{\mathbf{\Psi}}_{(j)} \circ \hat{\mathbf{\Sigma}}_{(j)})\mathbf{w}_{(j)}^{(t)} + 2\lambda \begin{pmatrix} \mathbf{w}_{\ell(j-1)} \\ \mathbf{0} \end{pmatrix}\right]}_{\triangleq \ddot{\mathbf{w}}_{(j)}^{(t)}}\Bigg) \tag{15}$$

The second step, called "Minimization", consists of minimizing the obtained function $g(.|\mathbf{w}^{(t)})$ to produce the iterate $\mathbf{w}^{(t+1)}$. The obtained form of the surrogate can be minimized using Lemma 2.

Lemma 2 *The solution of the following minimization problem*

$$\underset{\mathbf{w}\in\mathbb{T}_p}{\text{minimize}} \quad -Re(\mathbf{w}^H \ddot{\mathbf{w}})$$

is obtained at $\mathbf{w}^\star = \Phi_{\mathbb{T}}(\ddot{\mathbf{w}})$ *with* $\Phi_{\mathbb{T}} : x = re^{i\theta} \to e^{i\theta}$

The resulting MM algorithm is summed up in the table Algorithm 1.

Algorithm 1 MM algorithm for sliding IPL (13)

1: **Input**: $\hat{\mathbf{\Sigma}}_{(j)} \in \mathbb{C}^p$
2: Compute : $\mathbf{M} = 4(|\hat{\mathbf{\Sigma}}_{(j)}| \circ \hat{\mathbf{\Sigma}}_{(j)})$
3: **repeat**
4: Compute $\ddot{\mathbf{w}}_{(j)}^{(t)} = \mathbf{M}\mathbf{w}_{(j)} + 2\lambda \begin{pmatrix} \mathbf{w}_{\ell(j-1)} \\ \mathbf{0} \end{pmatrix}$
5: Update of $\mathbf{w}_{(j)}^{(t)} = \Phi_{\mathbb{T}}\{\ddot{\mathbf{w}}_{(j)}^{(t)}\}$
6: $t = t + 1$
7: **until** convergence
8: **Output**: $\hat{\mathbf{w}}_{(j)} = \mathbf{w}_{end} \in \mathbb{T}_p$

V. Real world experiments

To assess the performances of the proposed approach, we apply it to a real-world dataset. This allows for the validation of the proposed method in a real scenario.

A. Dataset

The dataset is composed of 30 Sentinel-1 SAR images acquired between $03/08/2019$ and $16/07/2020$ over the Mexico City. This city is one of the most densely populated in the world and has been subject of numerous studies, such as [17–20], due to the rapid urbanization it has undergone. As a result of this urbanization and the continuous population growth, the demand for potable water has significantly increased, leading to the extraction of water from aquifers. This practice has caused widespread ground deformation and subsidence across the city. The pre-processing of SAR images and the phase unwrapping (using SNAPHU) are done using Sentinel Application Platform (SNAP) software by European Space Agency (ESA) [21].

B. Performance and comparison

We compare our results with the offline COFI-PL approach, where tapering regularization is applied to the PO plug-in of the CM. This combination of the distance metric and the plug-in demonstrated optimal performance in phase estimation [6]. We also compare our results with the sequential approach proposed in [9], where we choose the same stack size $p = 5$ as in our approach. We do not compare the obtained results with those of the [12], as their results have demonstrated similar performances to the offline approach COFI-PL of [6]. We use the Structural SIMilarity index (SSIM) (measuring the similarity between two images) for the unwrapped interferograms[1] and the colinearity criterion [22] (evaluating the signal to noise ratio) for the wrapped interferograms.

Method	Colinearity	SSIM	Time
Sl-IPL	0.90	0.94	3.9 min
Sequential IPL [9]	0.84	0.85	17.1 min
COFI-PL [6]	0.91	Ref	92.4 min

TABLE I
QUANTITATIVE VALUES FOR THE EVALUATION OF THE ESTIMATED PHASES

In Fig. 3, it can be seen that the proposed approach (first and fourth column) yields similar results to the offline COFI-PL approach with BW-PO as a plug-in for the CM (second and fifth column). This observation is consistent with the colinearity and SSIM values obtained for both (wrapped and unwrapped phases) with both methods (Table I). The proposed approach (first and fourth column) yields better results than the Sequential Estimator proposed in [9] (third and last column), with better colinearity (better Signal-to-Noise Ratio (SNR)) and higher SSIM (closer resemblance to the offline approach, represented in the table by Ref).

C. Complexity and computation time

The complexity of these methods based on covariance fitting with the Frobenius distance depends on the number of images used, as it does not require costly mathematical operations, such as matrix inversion, which are common in most IPL algorithms [1–3, 23, 24]. The complexity of the offline approach COFI-PL is of the order $O(l^2)$, whereas that of the proposed approach is $O(p^2)$. The Sequential Estimator [9] has a complexity around $O(p^3 + i^3)$, where i denotes the number of compressed historical blocks, in other words the complexity of this approach depends not only on the number of new images, but also on images from the past, so at some point this i will become enormous. On a machine with a

[1]In InSAR, wrapped interferograms show phase values within a $-\pi$ to π range, resulting in a cyclic pattern due to phase ambiguity. In contrast, unwrapped interferograms resolve this ambiguity by converting phase into a continuous surface.

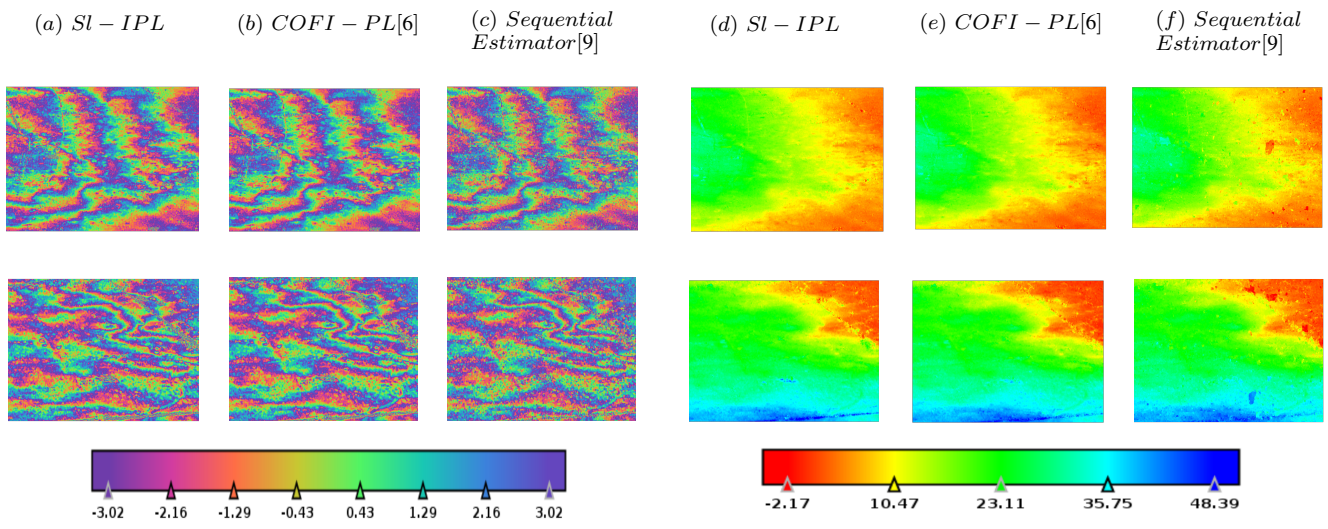

Fig. 3. The longest temporal baseline interferograms estimated by Sl-IPL, COFI-PL [6] and the Sequential Estimator [9] are presented, with the first three columns showing the wrapped phases and the second three columns displaying the unwrapped phases. Different patches are presented by line.

95−core CPU running at 2.2 GHz and 125 GB of RAM, where computations are executed in parallel across the cores, the proposed approach achieves significantly faster processing time than the offline COFI-PL approach and the Sequential Estimator. The computation time is provided in Table I.

VI. Conclusions

In this paper, we introduce a novel approach for SAR phase estimation that can incorporate new images based on covariance fitting approach in IPL. The proposed approach offers achieving comparable performance to the offline COFI-PL method. It offers reduced computation and processing time without the need to store past images, while still leveraging the information they provide. Our approach can be applied to any cost function and any plug-in along with regularization possibility. A real-world case study on the subsidence of Mexico City is conducted to demonstrate the relevance and effectiveness of our approach.

References

[1] A. Guarnieri and S. Tebaldini, "On the exploitation of target statistics for SAR interferometry applications," *IEEE Transactions on Geoscience and Remote Sensing*, vol. 46, no. 11, pp. 3436–3443, 2008.

[2] P. Vu, A. Breloy, F. Brigui, Y. Yan, and G. Ginolhac, "Robust Phase Linking in InSAR," *IEEE Transactions on Geoscience and Remote Sensing*, vol. 61, pp. 1–11, 2023.

[3] C. Wang, X. Wang, Y. Xu, Bochen Zhang, M. Jiang, S. Xiong, Q. Zhang, W. Li, and Q. Li, "A New Likelihood Function for Consistent Phase Series Estimation in Distributed Scatterer Interferometry," *IEEE Transactions on Geoscience and Remote Sensing*, vol. 60, pp. 1–14, 2022.

[4] N. Cao, H. Lee, and H. Jung, "Mathematical framework for phase-triangulation algorithms in distributed-scatterer interferometry," *IEEE Geoscience and Remote Sensing Letters*, vol. 12, no. 9, pp. 1838–1842, 2015.

[5] D. Minh and S. Tebaldini, "Interferometric Phase Linking: Algorithm, application, and perspective," *IEEE Geoscience and Remote Sensing Magazine*, vol. 11, no. 3, pp. 46–62, 2023.

[6] P. Vu, A. Breloy, F. Brigui, Y. Yan, and G. Ginolhac, "Covariance fitting interferometric phase linking: Modular framework and optimization algorithms," *IEEE Transactions on Geoscience and Remote Sensing*, vol. 63, pp. 1–18, 2025.

[7] Y. Bai, J. Kang, X. Ding, A. Zhang, Z. Zhang, and N. Yokoya, "LaMIE: Large-Dimensional Multipass InSAR Phase Estimation for Distributed Scatterers," *IEEE Transactions on Geoscience and Remote Sensing*, vol. 61, pp. 1–15, 2023.

[8] S. Zwieback, "Cheap, valid regularizers for improved interferometric phase linking," *IEEE Geoscience and Remote Sensing Letters*, vol. 19, pp. 1–4, 2022.

[9] H. Ansari, F. De Zan, and R. Bamler, "Sequential Estimator: Toward efficient InSAR time series analysis," *IEEE Transactions on Geoscience and Remote Sensing*, vol. 55, no. 10, pp. 5637–5652, 2017.

[10] D. El Hajjar, Y. Yan, G. Ginolhac, and M.N. El Korso, "Sequential phase linking: progressive integration of SAR images for operational phase estimation," in *IGARSS IEEE International Geoscience and Remote Sensing Symposium*. IEEE, 2024.

[11] D. El Hajjar, G. Ginolhac, Y. Yan, and M.N. El Korso, "Robust sequential phase estimation using multi-temporal sar image series," *IEEE Signal Processing Letters*, vol. 32, pp. 811–815, 2025.

[12] D. El Hajjar, G. Ginolhac, Y. Yan, and M.N. El Korso, "Sequential covariance fitting for insar phase linking," *arXiv preprint arXiv:2502.09248*, 2025.

[13] P. Vu, A. Breloy, F. Brigui, Y. Yan, and G. Ginolhac, "Covariance fitting based InSAR Phase Linking," in *IGARSS IEEE International Geoscience and Remote Sensing Symposium*. IEEE, 2023, pp. 8234–8237.

[14] G. Shevlyakov L and H. Oja, *Robust correlation: Theory and applications*, vol. 3, John Wiley & Sons, 2016.

[15] E. Ollila and A. Breloy, "Regularized tapered sample covariance matrix," *IEEE Transactions on Signal Processing*, vol. 70, pp. 2306–2320, 2022.

[16] Y. Sun, P. Babu, and D.P. Palomar, "Majorization-Minimization algorithms in signal processing, communications, and machine learning," *IEEE Transactions on Signal Processing*, vol. 65, no. 3, pp. 794–816, 2016.

[17] P. López-Quiroz, M-P. Doin, F. Tupin, P. Briole, and J-M Nicolas, "Time series analysis of mexico city subsidence constrained by radar interferometry," *Journal of Applied Geophysics*, vol. 69, no. 1, pp. 1–15, 2009.

[18] M-P Doin, P. Lopez-Quiroz, Y. Yan, P. Bascou, and V. Pinel, "Time series analysis of mexico city subsidence constrained by radar interferometry," in *EGU General Assembly Conference Abstracts*, 2010, p. 12031.

[19] B. Osmanoğlu, T. Dixon, S. Wdowinski, E. Cabral-Cano, and Y. Jiang, "Mexico city subsidence observed with persistent scatterer insar," *International Journal of Applied Earth Observation and Geoinformation*, vol. 13, no. 1, pp. 1–12, 2011.

[20] D. Ortiz-Zamora and A. Ortega-Guerrero, "Evolution of long-term land subsidence near mexico city: Review, field investigations, and predictive simulations," *Water Resources Research*, vol. 46, no. 1, 2010.

[21] European Space Agency (ESA), "SNAP," https://step.esa.int/main/toolboxes/snap.

[22] B. Pinel-Puysségur, R. Michel, and J-P Avouac, "Multi-link InSAR time series: Enhancement of a wrapped interferometric database," *IEEE Journal of Selected Topics in Applied Earth Observations and Remote Sensing*, vol. 5, no. 3, pp. 784–794, 2012.

[23] A. Ferretti, A. Fumagalli, F. Novali, C. Prati, F. Rocca, and A. Rucci, "A new algorithm for processing interferometric data-stacks: SqueeSAR," *IEEE transactions on geoscience and remote sensing*, vol. 49, no. 9, pp. 3460–3470, 2011.

[24] H. Ansari, F. De Zan, and R. Bamler, "Efficient phase estimation for interferogram stacks," *IEEE Transactions on Geoscience and Remote Sensing*, vol. 56, no. 7, pp. 4109–4125, 2018.